REAUSTENITISATION IN STEEL WELD DEPOSITS

J. R. Yang and H. K. D. H. Bhadeshia

University of Cambridge
Department of Materials Science and Metallurgy
Pembroke Street, Cambridge CB2 3QZ, U.K.

Abstract

The process of reaustenitisation in weld deposits, beginning with a microstructure of acicular ferrite and austenite, has been studied in order to enable the prediction of the reheated microstructure of welds. The transformation mechanism by which the original acicular ferrite formed is found to strongly influence the reaustenitisation process. The reverse $\alpha \rightarrow \gamma$ transformation does not occur immediately when the temperature is raised, even though the alloy may be in the $\alpha+\gamma$ phase field. Reaustenitisation only begins when the carbon concentration of the residual austenite exceeds its equilibrium carbon concentration. This is a direct consequence of the fact that the acicular ferrite transformation ceases before the lever rule is satisfied. A theory has been developed, which explains the experimental data, including the fact that the degree of reaustenitisation varies with temperature above the Ae3 curve.

Nomenclature

Braces are used exclusively to denote functional relations; x{T} therefore implies that T is the argument of the function x.

k_i	Partitioning coefficient for alloying element i
Δl_m	Maximum relative length contraction observed during isothermal reaustenitisation
T	Temperature
T_a	Temperature at which acicular ferrite forms
T_γ	Temperature of isothermal reaustenitisation
$T_{\gamma 1}$	Minimum T at which reaustenitisation commences
$T_{\gamma 2}$	Minimum T at which alloy becomes fully austenitic
V_γ	Equilibrium volume fraction of austenite
$\bar{x}$	Average carbon concentration of alloy
x_γ	Carbon concentration of austenite
x'_γ	Carbon concentration of residual austenite when the formation of acicular ferrite ceases
$x_{T'_o}$	Carbon concentration given by the T'_0 curve
x_{Ae3}	Carbon concentration given by the Ae3 curve
γ	Austenite
α	Ferrite

Introduction

The microstructure of the fusion zone of a multipass weld can be classified into two main components: (a) the primary microstructure obtained during cooling of the weld from the liquidus temperature which consists of allotriomorphic ferrite, Widmanstätten ferrite, acicular ferrite and very small amounts of "microphases" (i.e., martenisite, degenerate pearlite, retained austenite), and (b) the secondary microstructure, commonly called the reheated microstructure, obtained during the deposition of further weld metal. The thermal cycle experienced may just anneal the microstructure and cause recrystallisation and grain growth, or if the Ac_1 temperature is exceeded, it may reaustenitise to a degree depending on the thermodynamics and kinetics of reaustenitisation. The part which becomes austenitic then undergoes a series of transformations during the cooling part of the thermal cycle, the nature of the transformations depending on alloy chemistry, austenite grain size and morphology and cooling conditions amongst other factors.

Much work has recently been done on the prediction of the primary microstructure of welds using detailed phase transformation theory, and this has met with reasonable success (1-4).

Indeed, it is now possible to estimate quantitatively, the primary microstructure of arc welds as an aid to the design of welding consumables and procedures. However, there is no corresponding theory available for the reheated microstructure, which can form a substantial proportion of a multipass weld deposit.

This work is part of a programme on the theoretical design of welding consumables and deals specifically with the problem of reaustenitisation, and the factors influencing the temperature at which austenite first forms as a function of alloy chemistry, heating rate and starting microstructure. In order to establish a quantitative model for reaustenitisation, the work is initially limited to *isothermal* reaustenitisation experiments.

Experimental Procedures

Dilatometry

All dilatometry was performed on a Theta Industries high-speed dilatometer, which has a water cooled radio-frequency furnace of essentially zero thermal mass, since it is only the specimen which undergoes the programmed thermal cycle. The length transducer on the dilatometer was calibrated using pure platinum and pure nickel specimens of known thermal expansion characteristics. This enables rapid heating or cooling experiments. The dilatometer has been specially interfaced with a BBC/Acorn microcomputer so that length, time and temperature information can be recorded at microsecond intervals, and the data stored on a floppy disc. The information is then transferred to a mainframe IBM3081 computer for further analysis. Such a facility is essential for the present work since the transformations can occur at very rapid rates, and since a large number of experiments were conducted.

Specimens for dilatometry were in the form of 3mm diameter rods 15mm long, machined from the weld deposits with the cylinder axes parallel to the welding direction. The specimens were machined from regions far from the fusion line of the parent plate and are not affected by dilution from the parent material. To avoid surface nucleation and surface degradation, all specimens were plated with nickel (plating thickness $\approx$ 0.08mm) and all heat treatments were carried out in a helium gas environment. All experiments were conducted on specimens which had been homogenised at 1300^{o}C for 3 days, while sealed in quartz tubes containing a partial pressure of pure argon. The microstructure of the specimens before reaustenitisation was always acicular ferrite in a matrix of austenite.

Weld metal preparation

The welds were deposited using manual metal arc welding. The electrodes (4mm diameter) used were of a AWS-E10016-G type, the joint geometry being compatible with British Standard BS639 (similar to ISO2560), a geometry which gives large regions of weld metal free from dilution by the parent plate. All samples for the present work are removed from regions not influenced by dilution. The welding was carried out in the flat position using the stringer bead technique, the parent plate thickness being 20mm. The welding current and voltage used were 180A 23V (DC+) respectively, with an electrical energy input of about 2kJ/mm, the weld consisting of some 27 runs with 3 runs per layer. The interpass temperature was typically 250^{o}C.

The present study is connected with other work on high-strength weld deposits, and the electrodes for this purpose gave a deposit composition as follows:

Fe-0.06C-0.27Si-1.84Mn-2.48Ni-0.20Mo-0.0032O-0.01Al-0.02Ti, wt.%.

Transmission Electron Microscopy and Microanalysis

Thin foil specimens were prepared for transmission electron microscopy from 0.25mm thick discs slit from specimens used in the dilatometric experiments. The discs were thinned to 0.05mm by abrasion on silicon carbide paper and then electropolished in a twin jet electropolisher using a 5% perchloric acid, 25% glycerol and 70% ethanol mixture at ambient temperature, 60V.

The microscopy and microanalysis were conducted on a Philips EM400T transmission electron microscope operated at 120kV. An energy dispersive X-ray analysis facility was used for the microanalytical measurements, with the specimens held in a beryllium holder tilted from the normal by 35^{o}, which is the take-off angle. The X-ray count rate was optimised to about 200 counts/s over a livetime of about 100s. The data were analysed using the *LINK RTS 2 FLS* program for thin foil microanalysis; this corrects that data for atomic number and absorption and accounts for overlapping peaks by fitting standard profiles. Even though the probe diameter used was about 3nm, beam spreading due to scattering of electrons within the thin foil gave an estimated broadened beam diameter of $\approx$ 20nm.

Results and Discussion

The Nature of Acicular Ferrite

Before discussing the results in detail, it is necessary to state briefly some recent work (5,6) on the mechanism of acicular ferrite formation, particularly with respect to the thermodynamics of transformation. This provides a rational explanation for the design of the experiments and a basis for the interpretation of the results.

The composition of the alloy used is such that after welding, it gives a microstructure consisting mainly of acicular ferrite (volume fraction $\approx$ 0.9), with very little allotriomorphic ferrite and Widmanstätten ferrite (Fig. 1). The latter constituents only arise because of the presence of chemical segregation in the weld, which cools under non-equilibrium conditions. The high hardenability of this alloy (Fig. 1) is a major advantage for the present study because it allows the starting microstructure to be controlled with ease.

A thermodynamic investigation (5,6) has shown that the mechanism of transformation from austenite to acicular ferrite is the same as that for bainite: the plates grow by a diffusionless and displacive transformation mechanism (nucleation, although displacive, involves partitioning of carbon - Ref.8), and immediately after plate growth, carbon is partitioned into the residual

austenite. The transformation does not therefore obey the lever rule and exhibits a classical *incomplete reaction phenomenon* in which reaction ceases well before the residual austenite achieves its equilibrium carbon concentration. In fact, the transformation stops when the carbon concentration of the residual austenite (i.e., x_γ) reaches the T'_0 curve on the phase diagram.

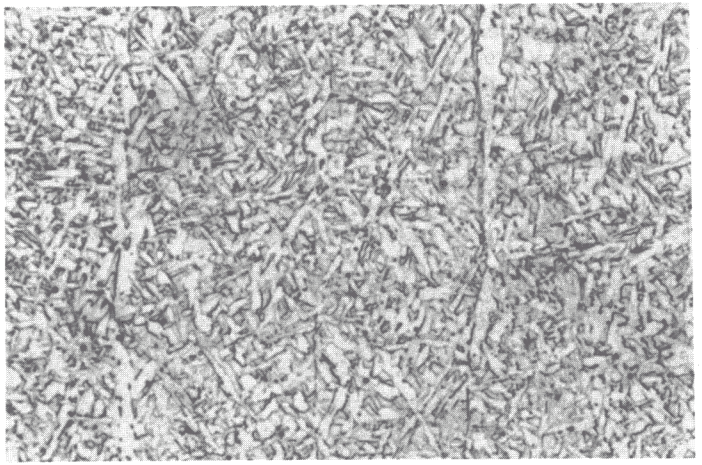

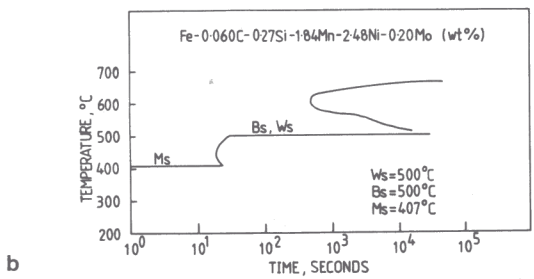

Figure 1 - (a) The primary microstructure of the weld deposit, consisting essentially of acicular ferrite, with very little allotriomorphic and Widmanstätten ferrite. (b) Calculated Time-Temperature-Transformation curve for a homogeneous alloy of the weld composition.

The T_0 curve, in a plot of temperature versus carbon concentration, represents all compositions where austenite and ferrite of the same composition have equal free energy (7-10). Diffusionless transformation is thermodynamically only possible if at the transformation temperature concerned, x_γ is less than the carbon concentration given by the T_0 curve. In fact, it is now known that the formation of acicular ferrite causes an invariant-plane strain (IPS) shape change in the transformed region. Consequently, allowance has to be made for the strain energy due to the IPS shape change. This strain energy amounts to about 400J/mol (5,6,8), and when this is accounted for, a T'_0 curve is defined such that diffusionless transformation is only possible if x_γ is less than x_T, the carbon concentration specified by the T'_0 curve for the isothermal transformation temperature concerned.

This mechanism of acicular ferrite formation explains many of its other features, such as the plate morphology, and the fact that the plates never cross austenite grain boundaries. Without going into further details, which are already published (5), the work indicates that acicular ferrite is really bainite, whose morphology differs from classical sheaf like bainite simply because acicular ferrite nucleates intragranularly at point sites, and is limited also by hard impingement with other neighbouring plates. Classical bainite sheaves form in pure alloys not containing large numbers of inclusions, where the bainite nucleates from austenite grain boundaries. Acicular ferrite requires the presence of inclusions to enable intragranular nucleation, and will only form when the austenite grain size is relatively large. Intragranular nucleation on inclusions, which has a higher activation energy compared with grain boundary nucleation so that the number of grain boundary sites must be minimised to obtain acicular ferrite. In fact, it has been shown (5) using light microscopy that on reaustenitisation and subsequent isothermal transformation, classical bainite forms in the present alloy if the austenite grain size is small, but acicular ferrite forms when the grain size is large. Fig. 2 provides striking transmission electron micrographs from specimens with varying austenite grain size which confirm the earlier work.

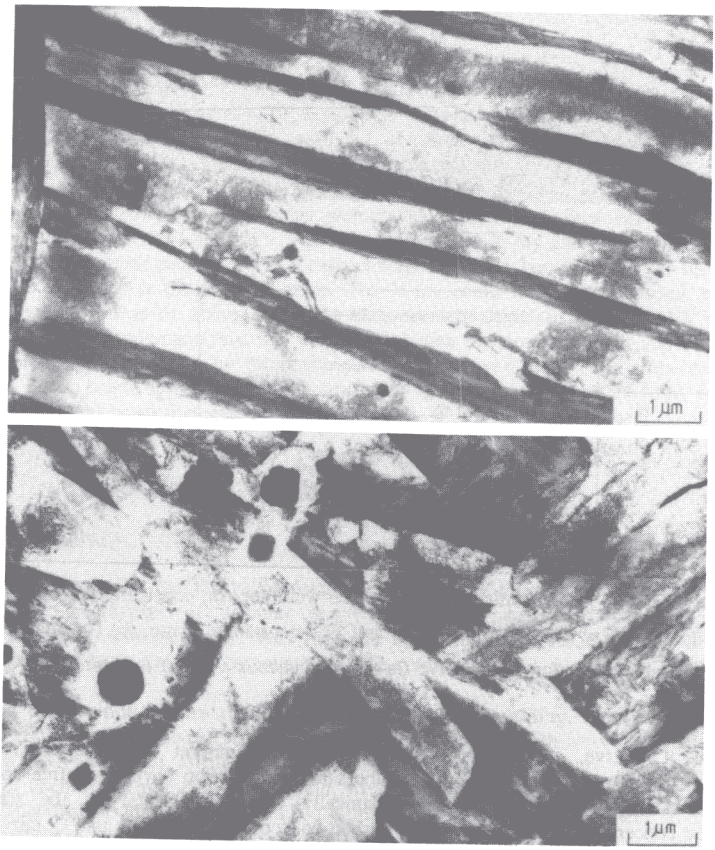

Figure 2 - Transmission electron micrographs. (a) Weld reaustenitised at 950°C for 10 min, isothermally transformed at 460°C for 30 min and water quenched. Shows classical sheaf of upper bainite. (b) Weld reaustenitised at 1200°C for 30 min and then transformed as in (a). Shows classical acicular ferrite.

Our aim was to study isothermal reaustenitisation, beginning with a microstructure consisting of acicular ferrite and austenite. For this reason, the experiments were carried out on weld specimens homogenised, austenitised at 1200°C for 30 min, isothermally transformed to acicular ferrite at a temperature T_a= 460°C for 30 min and then rapidly up-quenched to a temperature T_γ for isothermal reaustenitisation. The specimens were not cooled below 460°C, in order to avoid the martensitic decomposition of some or all of the residual austenite at that temperature. It should be noted that 30 mins at 460°C is more than adequate to allow the acicular ferrite transformation to terminate.

In addition, to avoid the *diffusional* decomposition of austenite during the up-quench from T_a, a sufficiently high up-quench rate has to be used during heating to T_γ. In these circumstances, reaustenitisation does not require the nucleation of austenite, just the growth of austenite. In the present study, the computer link to the dilatometer allowed high resolution monitoring of events during up-quenching, and for all the results reported here, there was no transformation during heating. A study involving the nucleation austenite will be reported separately. We note that the present results are relevant in any case, because the primary microstructure of welds often contains substantial amounts of retained austenite.

Isothermal Reaustenitisation

The results obtained from dilatometric experiments are presented in Fig. 3; the first detectable growth of austenite was found to occur at T_γ = 680°C. In all cases the transformation rate was initially rapid, but decreased with time so that the specimen length eventually stopped changing, as transformation ceased. If the maximum relative length change obtained at any T_γ is designated Δl_m, then Fig 4 shows that Δl_m increases as T_γ increases from 680°C to 760°C and then stays essentially constant with further increase in T_γ. It should be noted that a small amount of transformation occurred during the up-quench, when attempts were made to isothermally reaustenitise specimens at temperatures above 735°C. The transformation during the up-quench was recorded by the computer; it contributes to specimen length change, and a correction for this has been included in the data of Fig. 4. The correction is easy to make. During continuous heating, the specimen length varies linearly with temperature. If the low-temperature part of the curve (in a length versus temperature plot) is extrapolated to T_γ, the vertical difference between the extrapolated curve and the actual curve gives the length change due to transformation during the up-quench, which should be added to any length change due to isothermal transformation at T_γ

Since the temperature range covered is not very large, the results indicate that below 760°C, reaustenitisation is incomplete, the alloy becoming fully austenitic only above this temperature. Furthermore, the maximum degree of transformation to austenite increases from nearly zero at 680°C to complete reverse transformation at 760°C and above.

It is also seen from Fig. 3 that the rate of the reverse $\alpha \rightarrow \gamma$ transformation increases with T_γ

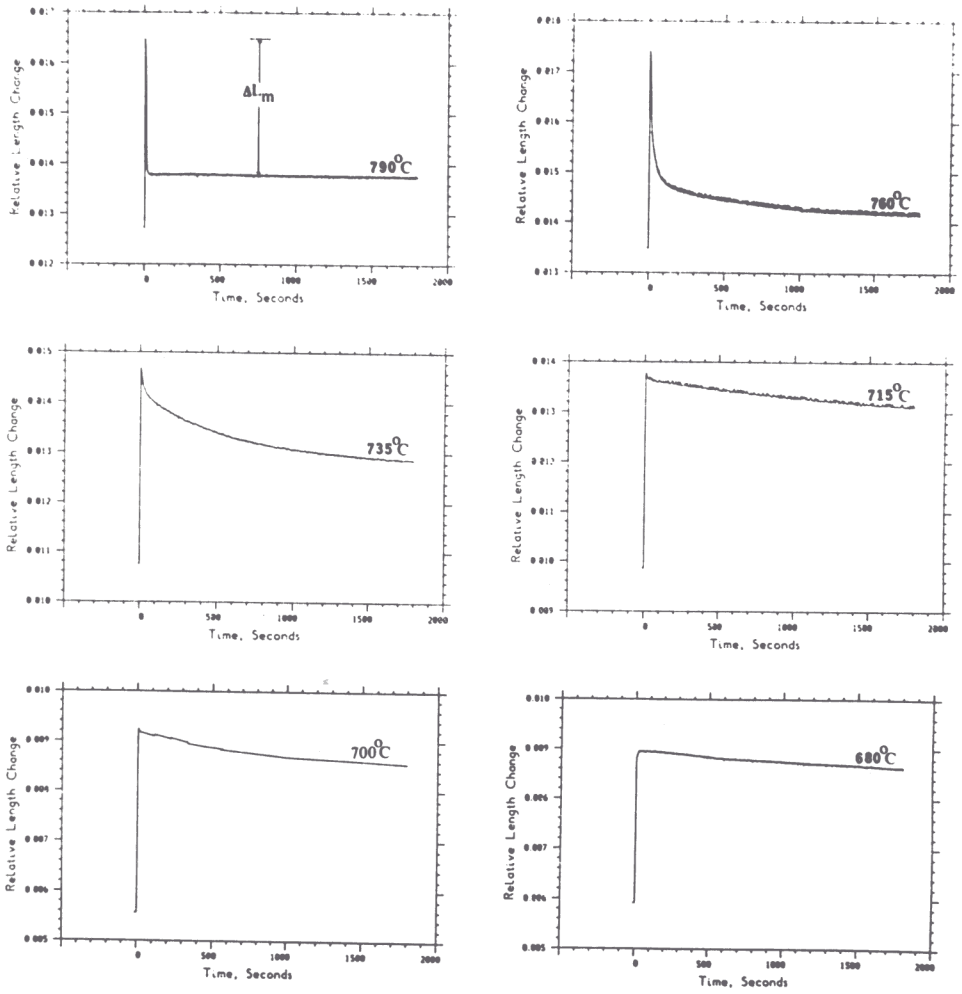

Figure 3 - Isothermal reaustenitisation experiments. The specimens were initially austenitised at 1200°C for 30 min, isothermally partially transformed to acicular ferrite at 460°C for 30 min and then rapidly up-quenched to an isothermal reaustenitisation temperature. Some transformation could not be avoided during the up-quench to temperatures above 735°C.

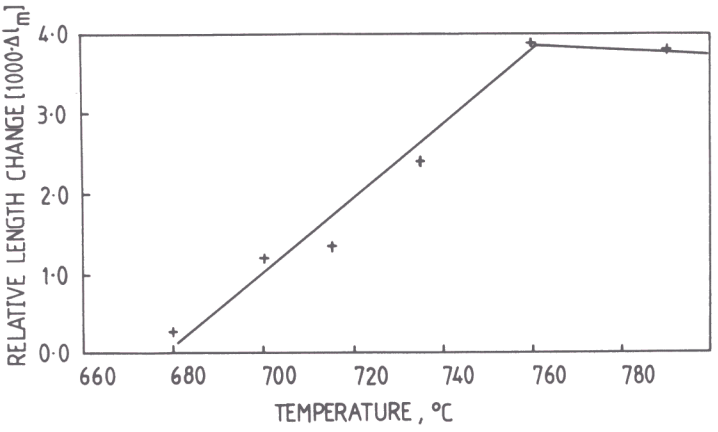

Figure 4 - A plot of the maximum relative length change Δl_m obtained at reaction termination, as a function of the isothermal reaustenitisation temperature T_γ

Table I. Microanalytical data (wt.%) for the γ and α during reaustenitisation.

Reaustenitisation		Mn	Mn	Ni	Ni
Temperature (^{o}C)	Time (min)	γ	α	γ	α
680	10	2.83	1.79	2.86	2.31
735	10	2.46	1.64	2.69	2.12
760	2	1.93	1.97	2.58	2.50
715	120	2.73	1.39	2.87	1.89
735	120	2.82	1.42	3.05	1.85
760	120	1.97	1.96	2.44	2.44

Microanalytical data

The results (Fig. 5, Table I) cover a range of times (t) at each T_γ, and a range of isothermal reaustenitisation temperatures. They show that for low T_γ, substitutional alloying additions redistribute during the $\alpha \rightarrow \gamma$ transformation, even at low t. For low transformation times, the degree of partitioning of alloying elements (as indicated by the deviation of the partition coefficient k_i from unity, where $k_i = x_i^\gamma / x_i^\alpha$) increases with decreasing T_γ. This is consistent with the fact that at low-T_γ, the redistribution of substitutional alloying elements is a thermodynamic necessity (11,12). As the driving force for reaustenitisation increases, the transformation tends towards paraequilibrium or negligible-partitioning-local equilibrium; this is illustrated clearly by the data for 760^oC, even for times as short as 2 minutes.

The concepts of paraequilibrium and local equilibrium have recently been reviewed (10). Paraequilibrium is a state of constrained equilibrium in which the substitutional lattice is configurationally frozen with respect to the transformation interface. Hence, even though the transformation is diffusional in nature, the ratio (atom fraction of substitutional element i/atom fraction of iron) is the same in α and γ. Thus, the chemical potentials of the substitutional elements are not equal in the two phases. Carbon which diffuses faster reaches equilibrium subject to this constraint. In negligible-partitioning-local-equilibrium (NPLE), equilibrium is maintained for all species at the transformation interface, but the concentration of substitutional elements is essentially the same in all phases.

The results also show that as t increases for a given T_γ, the partition coefficient k_i changes even though the volume fraction of austenite undergoes negligible change. This is strong evidence that the concentrations of alloying elements at the interface during the growth of austenite are not equilibrium concentrations.

These results are qualitatively consistent with the dilatometric data; one of the factors responsible for the increased rate of transformation at high T_γ is the fact that the degree of redistribution of alloying elements during transformation decreases with increasing T_γ. The results emphasize that although the states of local equilibrium or paraequilibrium are for convenience often assumed to define the compositions at the interface during diffusion-controlled growth, an infinite number of other possibilities exist for multicomponent alloys (10). All compositions of austenite which allow a reduction in free energy during growth can in principle form from ferrite, giving rise to situtations in which one or more of the elements is trapped by the moving interface; trapping implies an increase in he chemical potential of that element during transfer across the interface. The *prediction* of compositions at the interface is then a formidable theoretical problem which cannot be addressed until detailed information on interface mobility becomes available. On the other hand, any system must eventually tend towards equilibrium, so that the limiting composition of austenite can easily be calculated; this is the approach adopted in the present work.

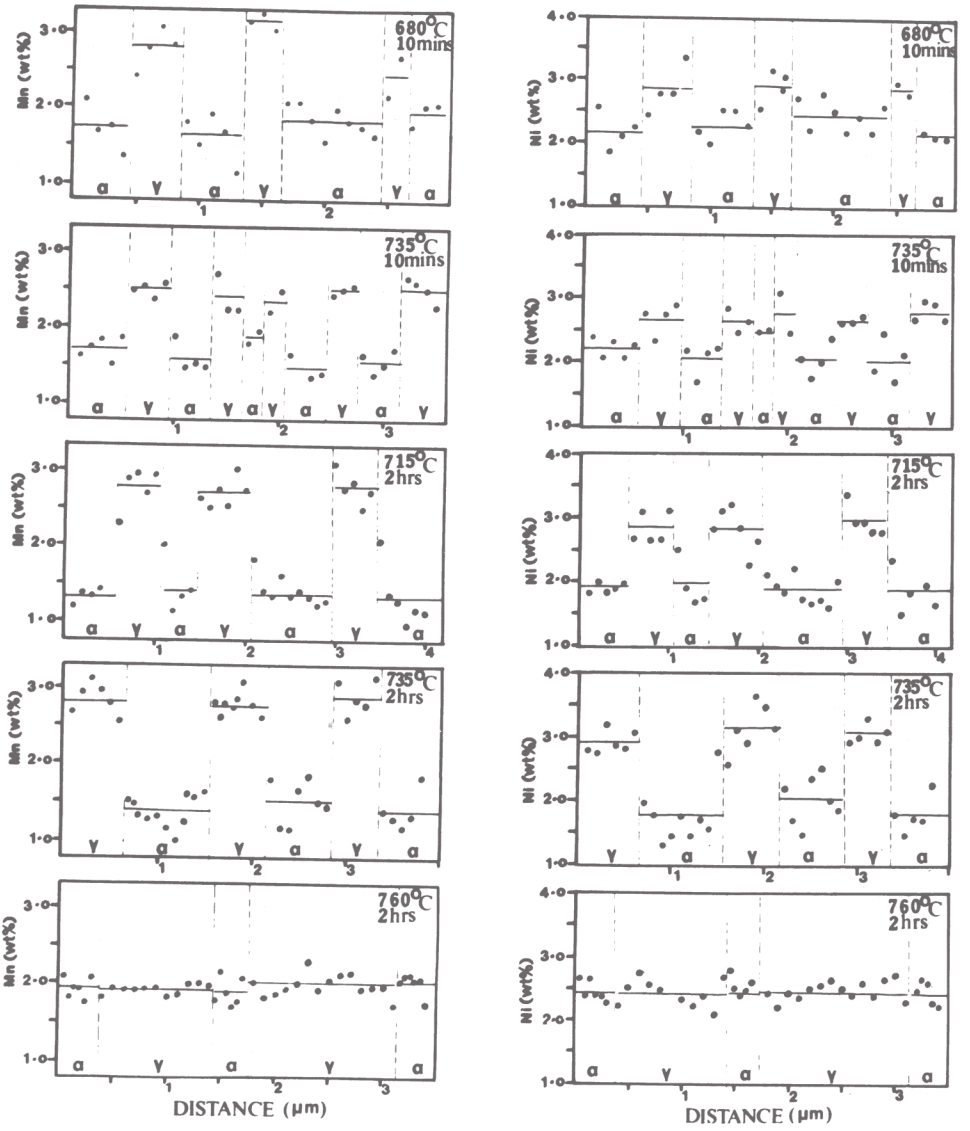

Figure 5 - Microanalytical data obtained using energy dispersive X-ray analysis on a transmission electron microscope.

Theoretical analysis

Here we present a model for the interpretation of the observations on reaustenitisation from a mixture of acicular ferrite and austenite. Since after the diffusionless growth of acicular ferrite, carbon is rapidly and spontaneously redistributed into the residual austenite with an accompanying reduction in free energy, the $\alpha_a \rightarrow \gamma$ transformation in its original form is irreversible. The problem of reaustenitisation is therefore considerably different from the case of reverse transformation from martensite to austenite in for example, shape memory alloys.

We have noted that the formation of acicular ferrite ceases prematurely during isothermal transformation when the carbon content of the residual austenite reaches the T'_0 curve (the phase diagram for the present alloy is presented in Fig. 6). It follows that the carbon concentration x'_γ of the austenite when the formation of acicular ferrite ceases at T_a, is given by (point marked **a** in Fig. 6):

$$x'_\gamma = x_{T'_o}\{T_a\} \qquad .....(1)$$

Furthermore, we note that:

$$x'_\gamma << x_{Ae3}\{T_a\} \qquad .....(2)$$

where $x_{Ae3}\{T_a\}$ is marked **b** in Fig. 6.

Thus, although the formation of *acicular ferrite* ceases at T_a, because $x'_\gamma << x_{Ae3}\{T_a\}$, the driving force for austenite to transform *diffusionally* to ferrite is still negative. Another way of expressing this is to say that the volume fraction of acicular ferrite present when its formation ceases at T_a is much less than required by the lever rule. In fact, this remains the case until the temperature T is high enough (i.e., $T=T_{\gamma 1}$) to satisfy the equation:

$$x'_\gamma = x_{Ae3}\{T_{\gamma 1}\} \qquad .....(3)$$

Hence, reaustenitisation will first occur at a temperature $T_{\gamma 1}$, as indicated on Fig. 6 (marked **c**), and as observed experimentally. Note that this is a direct consequence of the mechanism of the acicular ferrite transformation, which does not allow the transformation to reach completion. If this were not the case, then the lever rule demands that the temperature need only be raised infinitesimally above T_a in order for the reverse $\alpha \rightarrow \gamma$ transformation to be thermodynamically possible!

The theory goes further than explaining just the temperature at which the reverse transformation should begin. It also predicts that at any temperature T_γ greater than $T_{\gamma 1}$, the reverse $\alpha \rightarrow \gamma$ transformation should cease as soon as the residual austenite carbon concentration (initially x'_γ) reaches the Ae3 curve, i.e., when

$$x_\gamma = x_{Ae3}\{T_\gamma\} \quad \text{.....(4)}$$

with the equilibrium volume fraction of austenite (at the temperature T_γ), $V_\gamma\{T_\gamma\}$, being given by:

$$V_\gamma\{T_\gamma\} = \bar{x}/x_{Ae3}\{T_\gamma\} \quad \text{.....(5)}$$

assuming that the carbon concentration of ferrite is negligible and that $x_{Ae3}\{T_\gamma\}>\bar{x}$. When $x_{Ae3}\{T_\gamma\}=\bar{x}$, the alloy eventually becomes fully austenitic (point **d** , Fig. 6), and if this condition is satisfied at $T_\gamma=T_{\gamma 2}$, then for all $T_\gamma>T_{\gamma 2}$, the alloy transforms completely to austenite.

These concepts immediately explain the dilatometric data in which the degree of $\alpha\rightarrow\gamma$ transformation increases (from ≈ zero at 680°C) with the temperature of isothermal reaustenitisation, until the temperature 760°C=$T_{\gamma 2}$ where the alloy transforms completely to austenite.

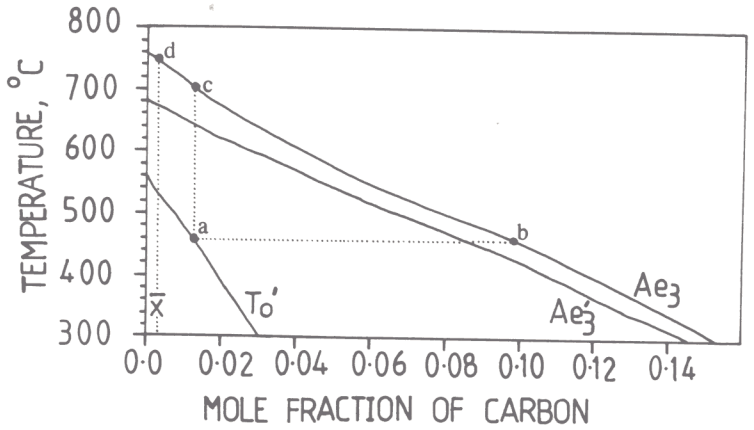

Figure 6 - Phase diagram showing the Ae3, Ae3', T_0 and T_0' curves for a Fe-0.27Si-1.84Mn-2.48Ni-0.20Mo wt.% alloy. The Ae3', T_0 and T_0' curves are calculated as in Refs.7,8, and the Ae3 curve is calculated as in Ref.13.

Conclusions

Reaustenitisation of a weld deposit, beginning with a microstructure of just acicular ferrite and bainite has been studied under isothermal conditions and in circumstances where the nucleation of austenite is not necessary. The reverse transformation from acicular ferrite to austenite does not happen immediately the temperature is raised (above that at which the acicular ferrite formed), even though the alloy is within the $\alpha+\gamma$ phase field.

This is because acicular ferrite plates grow by a diffusionless displacive transformation mechanism (similar to that of bainite) which ensures that the transformation ceases prematurely, before the residual austenite achieves its equilibrium composition. Hence, reaustenitisation only occurs when the alloy is heated to a temperature where the carbon concentration of the residual austenite exceeds its equilibrium concentration.

Complete transformation to austenite only occurs at a temperature where the alloy composition equals the austenite equilibrium composition. However, at all intermediate temperatures, the reverse $\alpha \rightarrow \gamma$ transformation terminates before the alloy becomes fully austenitic, with the volume fraction of austenite increasing with increasing T_γ.

The work has led to a theory for reaustenitisation which explains most of the experimental results, but which as yet does not address the detailed kinetics of reaustenitisation. The model predicts accurately the temperature at which reaustenitisation should begin and the degree of transformation to austenite as a function of the isothermal reaustenitisation temperature. All this is in turn a function of the temperature at which the original acicular ferrite itself formed.

Acknowledgments

The authors are grateful to the Chinese Ministry of Education for financial support, to ESAB for the provision of weld samples, to Professor D. Hull for the provision of laboratory facilities, and to G. Barritte, P. Judson and L. -E. Svensson for helpful discussions throughout the course of this work.

References

1. H. K. D. H. Bhadeshia, L.-E. Svensson and B. Gretoft, "A Model for the Development of Microstructure in Low-Alloy Steel Weld Deposits," Acta Metall., 33 (1985) 1271-1283.

2. L.-E. Svensson, B. Gretoft and H. K. D. H. Bhadeshia, "An Analysis of the Cooling Curves from the Fusion Zone of Steel Weld Deposits," Scand. J. Metall., 15 (1986) 97-103.

3. L.-E. Svensson, B. Gretoft and H. K. D. H. Bhadeshia, " Computer-Aided Design of Electrodes for Manual Metal Arc Welding," Computer Technology in Welding, (Welding Institute, Abington, Cambridge), in press.

4. H. K. D. H. Bhadeshia, L.-E. Svensson and B. Gretoft, "Prediction of the Microstructure of the Fusion Zone of Multicomponent Steel Weld Deposits," Advances in Welding Research, ed. S. A. David, (Metals Park, OH: American Society for Metals, 1987), 225-229.

5. J. R. Yang and H. K. D. H. Bhadeshia, "Thermodynamics of the Acicular Ferrite Transformation," Advances in Welding Research, ed. S. A. David,

(Metals Park, OH: American Society for Metals, 1987), 187-191

6. M. Strangwood and H. K. D. H. Bhadeshia, "Mechanism of Acicular Ferrite Formation in Steel Weld Deposits," Advances in Welding Research, ed. S. A. David, (Metals Park, OH: American Society for Metals, 1987), 209-213.

7. H. K. D. H. Bhadeshia and D. V. Edmonds, "The Mechanism of Bainite Formation in Steels," Acta Metall., 28 (1980) 1265-1273.

8. H. K. D. H. Bhadeshia, "A Rationalisation of Shear Transformations in Steels," Acta Metall., 29 (1981) 1117-1130.

9. H. K. D. H. Bhadeshia, "Bainite: Overall Transformation Kinetics," J. de Physique, C4-43 (1982) 443.

10. H. K. D. H. Bhadeshia, "The Diffusional Formation of Ferrite in Iron and its Alloys," Prog. in Mat. Sci., 29 (1985) 321-386.

11. G. R. Speich, V. A. Demarest and R. L. Miller, "Formation of Austenite During Intercritical Annealing of Dual-Phase Steels," Metall. Trans., 12A (1981) 1419-1428.

12. J. B. Gilmour, G. R. Purdy and J. S. Kirkaldy, "Thermodynamics Controlling the Proeutectiod Ferrite Transformation in Fe-C-Mn," Metall. Trans., 3 (1972) 1455-1469.

13. A. A. B. Sugden and H. K. D. H. Bhadeshia, Unpublished research based on the method of J. S. Kirkaldy, B. A. Thomson and E. Baganis, "Hardenability Concepts with Applications to Steel", Ed. D. V. Doane and J. S. Kirkaldy, pub. ASM, Warrendale, U. S. A., 1977, p. 82.